Available online at www.sciencedirect.com
SCIENCE DIRECT®
Inorganica Chimica Acta 357 (2004) 3510–3516
Inorganica Chimica Acta
www.elsevier.com/locate/ica

Synthesis, characterization and crystal structures of homo- and hetero-substituents containing *trans* six-coordinate tin(IV) complexes of H_2tmtaa (5,14-dihydro-6,8,15,17-tetramethyldibenzo[*b,i*][1,4,8,11]tetraazacyclotetradecine), and the solid state NMR spectra study of ^{119}Sn ☆

Xuan Shen *, Akio Nakashima, Kazunori Sakata *, Mamoru Hashimoto

Department of Applied Chemistry, Faculty of Engineering, Kyushu Institute of Technology, 1-1 Sensui-cho, Tobata-ku, Kitakyushu 804-8550, Japan

Received 4 January 2004; accepted 1 May 2004
Available online 9 June 2004

Abstract

The reaction of Sn(tmtaa)Cl_2 (H_2tmtaa = 5,14-dihydro-6,8,15,17-tetramethyldibenzo[*b,i*][1,4,8,11]tetraazacyclotetradecine) and ammonium thiocyanate or sodium azide under a mild condition resulted in *trans* six-coordinate tmtaa tin(IV) complexes, Sn(tmtaa)X_2 (X = NCS, **1**; X = N_3, **2**). However, the treatment of Sn(tmtaa)Cl_2 and sodium picrate produced Sn(tmtaa)(Cl)(OC_6H_2(2,4,6-3NO_2)) (**3**). Only one chloro atom of Sn(tmtaa)Cl_2 was substituted because of low nucleophilicity of the 2,4,6-trinitrophenolic anion in **3**. Furthermore, because of the steric hindrance between the 2,4,6-trinitrophenolic group and the tmtaa ligand, which has a non-planar, saddle-shaped conformation, two chloro atoms cannot be substituted by two 2,4,6-trinitrophenolic groups simultaneously. All complexes were characterized by IR spectra, UV spectra, mass spectra, NMR spectra and elemental analyses, as well as DSC measurements. X-ray crystal structures of **1** and **3** reveal that the complexes retain the characteristic saddle-shaped configuration of H_2tmtaa but have adopted the *trans* geometry. Solid state ^{119}Sn NMR spectroscopy was used to study the bonding environment in the series of six-coordinate *trans* Sn(IV) tmtaa complexes. It can be found that the ^{119}Sn chemical shifts of the Sn(IV) tmtaa complexes are almost not influenced by the substituents.

Keywords: Homo- and hetero-substituents; *Trans* six-coordinate complexes; Tin(IV) tmtaa complexes; Crystal structures; Solid state ^{119}Sn NMR spectra

1. Introduction

5,14-Dihydro-6,8,15,17-tetramethyldibenzo[*b,i*][1,4,8,11]tetraazacyclotetradecine, abbreviated as H_2tmtaa (Fig. 1), is a macrocyclic compound of a 14-membered ring and has a structure and properties similar to porphyrins and phthalocyanines. It also features important differences from porphyrins and phthalocyanines such as a smaller N_4 coordination cavity 'hole size' and typically possesses a non-planar, saddle-shaped conformation. The similarity of H_2tmtaa to the porphyrins and phthalocyanines means that these synthetic macrocycles are of bioinorganic relevance, while their distinctive individual characteristics make them interesting ligands in their own right. Syntheses, properties and structures of transition and main group metals tmtaa complexes were compiled by Cotton and Czuchajowska [1] and Mountford [2]. In the last decade, tmtaa complexes of Group 14 elements, especially germanium and tin, have enjoyed a resurgence of interest [3–9]. We have also reported the preparation,

☆ Supplementary data associated with this article can be found, in the online version, at doi:10.1016/j.ica.2004.05.011.

* Corresponding authors. Tel.: +81-93-884-3307/3331; fax: +81-93-884-3300.
E-mail addresses: chinsenjp@yahoo.co.jp (X. Shen), sakata@che.kyutech.ac.jp (K. Sakata).

0020-1693/$ - see front matter © 2004 Elsevier B.V. All rights reserved.
doi:10.1016/j.ica.2004.05.011

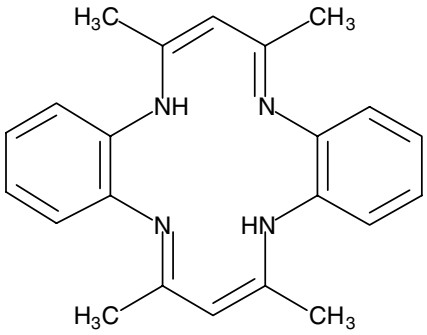

Fig. 1. Suggested structure of H_2tmtaa.

characterization and structures of tmtaa complexes of germanium in the +IV oxidation state recently [10,11]. In those theses, chloro-bridged dinuclear tmtaa germanium (IV) complex and *trans* six-coordinate tmtaa germanium (IV) complexes with homo- and hetero-substituents were reported. Herein, as extension of our research, we further report the investigations into a number of derivatives of other Group 14 element, tin, in the +IV oxidation state, including homo- and hetero-substituents *trans* six-coordinate tmtaa complexes. Additionally, the properties of solid state ^{119}Sn NMR spectra in the tmtaa complexes are also investigated.

2. Experimental

2.1. Materials

All analytical grade chemicals were purchased commercially and used without further purification. All solvents were distilled under a nitrogen atmosphere. Sn(tmtaa)Cl_2 is prepared according to the literature method [6].

2.2. Physical measurements

Elemental analyses were performed on a Yanaco CHN corder MT-3. IR spectra (4000–400 cm^{-1}) were recorded on a JASCO FT/IR-400 spectrophotometer in KBr pellets at room temperature. Ultraviolet and visible spectra were recorded on a Shimadzu UV-200S double beam spectrophotometer in chloroform at room temperature. DSC data were obtained using a Shimadzu DSC-50 differential calorimeter. ^{1}H NMR measurements were taken on a BRUKER AVANCE-400 in chloroform-d ($CDCl_3$), and chemical shifts were given in ppm relative to tetramethylsilane as an internal reference standard. Cross polarization magic angle spinning (CPMAS) NMR spectra were recorded on a BRUKER MSL300 spectrometer at Larmor frequencies $\mu_0/2\pi$ of 111.9 MHz for ^{119}Sn. ^{119}Sn chemical shielding is referenced to the ^{119}Sn resonance of tetramethyltin ($SnMe_4$) at 0 ppm and potassium stannate trihydrate ($K_2SnO_3 \cdot 3H_2O$), which shift appeared at −569 ppm, was used as secondary references.

Suitable crystals of **1** and **3** were mounted on glass fibers. All measurements were made on a Rigaku AFC7R diffractometer with graphite monochromated Mo Kα radiation ($\lambda = 0.71069$ Å) and a rotating anode generator. The structures of **1** and **3** were solved by direct methods [12] and expanded using Fourier techniques [13]. All non-hydrogen atoms were refined with anisotropic thermal parameters. Most of the hydrogen atoms were located in calculated positions and/or in positions found from difference Fourier maps. Crystal data and details associated with data collection are summarized in Table 1.

2.3. Synthesis of Sn(tmtaa)$(NCS)_2$ (*1*)

A solution of ammonium thiocyanate (0.030 g, 0.394 mmol) in methanol (5 ml) was added dropwise to a solution of Sn(tmtaa)Cl_2 (0.100 g, 0.188 mmol) in methanol (20 ml) under a nitrogen atmosphere. After being refluxed for 12 h, a product precipitated as a red microcystalline solid. The product was collected by filtration and washed thoroughly with methanol, and then was recrystallized from toluene/dichloromethane (1:4 vol/vol) to give red crystals suitable for X-ray diffraction. Yield: 0.095 g (88%). *Anal.* Calc. for Sn(tmtaa)$(NCS)_2$ ($C_{24}H_{22}N_6S_2Sn$): C, 49.93; H, 3.84; N, 14.56. Found: C, 50.01; H, 3.80; N, 14.44%. m.p.: 395–396 °C (DSC). IR (KBr pellet, cm^{-1}): 2047 (C≡N), 1511, 1456, 1391 (C=C, C=N). UV–Vis ($CHCl_3$, λ_{max}/nm): 386 (s), 430 (m). FAB-MS: $m/z =$ 518 (M − NCS), 460 (M − 2NCS). Solid state ^{119}Sn NMR: δ −432.

2.4. Synthesis of Sn(tmtaa)$(N_3)_2$ (*2*)

After Sn(tmtaa)Cl_2 (0.100 g, 0.188 mmol) was dissolved in methanol (20 ml) completely under a nitrogen atmosphere, a methanol solution (5 ml) of sodium azide (0.025 g, 0.385 mmol) was added dropwise. The solution was refluxed for 12 h and then was cooled to room temperature. After being filtered, the solution was reduced to half by evaporating. The product precipitated when the solution was cooled to room temperature again. The product was collected by filtration and washed thoroughly with methanol, and then was recrystallized from acetonitrile to give red microcrystalline solid. Yield: 0.078 g (76%). *Anal.* Calc. for Sn(tmtaa)$(N_3)_2$ ($C_{22}H_{22}N_{10}Sn$): C, 48.47; H, 4.07; N, 25.69. Found: C, 48.21; H, 4.16; N, 25.86%. m.p.: 366–368 °C (DSC). IR (KBr pellet, cm^{-1}): 2075 (NNN), 1523, 1465, 1388 (C=C, C=N). UV–Vis ($CHCl_3$, λ_{max}/

Table 1
Crystal data, data collection and refinement parameters for complexes **1** and **3**

Complex	**1**	**3**
Empirical formula	$C_{24}H_{22}N_6S_2Sn_1$	$C_{28}H_{24}Cl_1N_7O_7Sn_1 \cdot CH_3CN$
Formula weight	577.29	765.74
Crystal color, habit	red, block	red, chunk
Crystal dimensions	$0.10 \times 0.10 \times 0.10$ mm	$0.20 \times 0.30 \times 0.40$ mm
Crystal system	monoclinic	triclinic
Space group	$P2_1/n$(#14)	$P\bar{1}$(#2)
Number of reflections used for unit cell determination (2θ range)	25 (20.2 27.4°)	25 (21.3 31.0°)
Lattice parameters		
a (Å)	13.055(2)	10.416(2)
b (Å)	12.587(2)	16.417(3)
c (Å)	14.687(2)	9.3955(9)
α (°)	98.938(10)	
β (°)	92.20(1)	92.98(1)
γ (°)	89.65(2)	
V (Å^3)	2411.8(6)	1585.0(5)
Z value	4	2
$F(000)$	1160.00	772.00
D_{calc} (g/cm^3)	1.590	1.604
Radiation	Mo Kα ($\lambda = 0.71069$ Å) graphite monochromated	Mo Kα ($\lambda = 0.71069$ Å) graphite monochromated
Temperature (°C)	20.0	20.0
Scan type	$\omega - 2\theta$	$\omega - 2\theta$
$2\theta_{max}$	56.0°	56.0°
Number of reflections measured		
Total	6356	8068
Unique	5830 ($R_{int} = 0.067$)	8064 ($R_{int} = 0.022$)
Residuals: R; Rw	0.119; 0.163	0.128; 0.229
Residuals: R_1	0.056	0.070
Goodness-of-fit indicator	1.24	1.56
Maximum shift/error in final cycle	0.000	0.000

nm): 385 (s), 425 (m). FAB-MS: $m/z = 502$ ($M - N_3$), 460 ($M - 2N_3$). Solid state ^{119}Sn NMR: δ −436.

2.5. Synthesis of Sn(tmtaa)(Cl)(OC_6H_2(2,4,6-3NO_2)) · CH_3CN (**3**)

A solution of sodium picrate (0.113 g, 0.450 mmol) in methanol (5 ml) was added dropwise to a solution of Sn(tmtaa)Cl_2 (0.100 g, 0.188 mmol) in methanol (20 ml) under a nitrogen atmosphere. After being refluxed for 12 h, the solution was cooled to room temperature and was filtrated. Evaporating the filtrate resulted in red powder. Red crystals containing one molecule of acetonitrile, which were suitable for X-ray diffraction, were obtained by recrystallizating the powder from acetonitrile. Yield: 0.123 g (90%). *Anal.* Calc. for Sn(tmtaa)(Cl)(OC_6H_2(2,4,6-3NO_2))·CH_3CN ($C_{28}H_{24}ClN_7O_7Sn \cdot CH_3CN$): C, 47.05; H, 3.55; N, 14.63. Found: C, 47.16; H, 3.45; N, 14.78%. m.p.: 345-346 °C (DSC). IR (KBr pellet, cm^{-1}): 1582, 1488, 1457, 1397 (C═C, C═N). UV–Vis ($CHCl_3$, λ_{max}/nm): 390 (s), 420 (sh). FAB-MS: $m/z = 495$ ($M - OC_6H_2(NO_2)_3$), 460 ($M - Cl–OC_6H_2(NO_2)_3$). Solid state ^{119}Sn NMR: δ −415.

3. Results and discussion

3.1. Synthesis and characterization

The reaction of free base H_2tmtaa with $SnCl_4$ under mild condition resulted in Sn(tmtaa)Cl_2 [6]. Because of +IV oxidation state of the central metal and a *trans* six-coordinate geometry, Sn(tmtaa)Cl_2 shows great reactivity at the axial position. The substituting reaction of a methanol solution of Sn(tmtaa)Cl_2 with two equivalents of ammonium thiocyanate or two equivalents of sodium azide in methanol under mild condition (in a nitrogen atmosphere, refluxing) yielded new *trans* six-coordinate tin(IV) tmtaa complexes, Sn(tmtaa)$(NCS)_2$ (**1**) or Sn(tmtaa)$(N_3)_2$ (**2**). **1** and **2** were characterized by IR spectra, UV spectra, mass spectra, NMR spectra and elemental analyses, as well as DSC measurements. In the IR spectrum of **1**, the C≡N stretching band of NCS group was observed at 2047 cm^{-1}, while the NNN stretching band of the azido group in **2** appeared at 2075 cm^{-1} in its IR spectrum. The X-ray crystal structure of **1** shows an approximately octahedral coordination geometry with *trans* configuration. Analysis of the structure shows that it is nitrogen atom that coordinates to

the central metal, while it is not sulfur atom. The spectra data of **2** are similar to those of **1**, so that the structure of **2** should be analogous to that of **1**.

Until now, investigations into the interaction of tmtaa units and axial substituents containing aromatic groups in Group 14 elements tmtaa complexes have not been extensively developed. However, several titanium, zirconium, ruthenium and iron tmtaa complexes containing aromatic rings in the axial positions, which show very interesting configurations, have been reported [14–19]. In our work, though we changed the molar rate of $Sn(tmtaa)Cl_2$ and sodium picrate from 1:2 to 1:5, only one kind of tin tmtaa complexes, $Sn(tmtaa)(Cl)(OC_6H_2(2,4,6\text{-}3NO_2))$ (**3**), in which only one chloro atom was substituted, was obtained. This may be due to low nucleophilicity of the 2,4,6-trinitrophenolic anion. Furthermore, because of the steric hindrance between the 2,4,6-trinitrophenolic group and the tmtaa ligand, which has a non-planar, saddle-shaped conformation, two chloro atoms cannot be substituted by two 2,4,6-trinitrophenolic groups simultaneously. The X-ray crystal structure of **3** shows that the complex keeps the *trans* configuration and a chloro atom and a 2,4,6-trinitrophenolic group are in two sides of tmtaa ligand. Because of the interaction of 2,4,6-trinitrophenolic group and tmtaa unit, the aromatic ring in 2,4,6-trinitrophenolic group is not vertical to the N_4 plane of tmtaa.

3.2. Mass spectra

In the FAB^+ mass spectra of starting compound, $Sn(tmtaa)Cl_2$, no molecular ion peaks were observed, but only the peaks of major fragments corresponding to $[M-Cl]^+$ and $[M-2Cl]^+$ were observed [6]. This was also observed in our work. FAB^+ mass spectra of all complexes show the peaks of major fragments corresponding to molecule minus one and two substituents. This suggests that the substituents in *trans* positions may be easily cleaved in FAB^+ mass measurements.

3.3. ^1H NMR Spectra

Complexes **1**–**3** give well-resolved ^1H NMR spectra. ^1H NMR data for $Sn(tmtaa)Cl_2$ and **1**–**3** are listed in Table 2. The aromatic protons, which appear as a broad singlet at δ 6.98 ppm in the ^1H NMR spectrum of H_2tmtaa in $CDCl_3$ solution [20], separate into two multiplets in all the spectra. The signals of methine and methyl groups are all singlets. However, comparing with starting compound, the signals of **1**–**3** shift a little to upfield or downfield. This seems to indicate that the interactions between substituted groups and tmtaa units are different. For example, in the spectrum of $Sn(tmtaa)Cl_2$, the signals of methine and methyl groups appeared at δ 5.13 and 2.48 ppm, respectively. However, in the spectrum of **1**, the signals of methine and methyl groups appeared at δ 5.15 and 2.49 ppm, respectively, shifting a little to downfield. This may suggest that the interaction between NCS groups and tmtaa in **1** is stronger than the interaction between Cl groups and tmtaa in $Sn(tmtaa)Cl_2$. If stronger interaction appears between tmtaa and substituted groups, the protons electron cloud of tmtaa is attracted by substituted groups and the density of electron cloud becomes lower and lower. Thus, the proton signals shift to downfield in ^1H NMR spectra. This can also be observed in other complexes. Besides proton signals of tmtaa are observed, aromatic protons of substituted groups in **3** appear as singlet at δ 8.70 ppm.

3.4. Solid state NMR spectra of tin(IV)

The use of ^{119}Sn NMR spectroscopy has proven to be an invaluable structural probe in all areas of tin chemistry [21]. A large body of data is now available [22] which demonstrates that ^{119}Sn NMR studies provide accurate, relatively easily obtainable information on the bonding to the tin atom. In many cases, the most important spectroscopic parameter available from these studies is the value of the chemical shift (δ). While much

Table 2
^1H NMR (400 MHz)[a] and ^{119}Sn solid state NMR (111.9 MHz)[b] spectroscopic data for $Sn(tmtaa)Cl_2$ and complexes **1**–**3**

Complex	^1H NMR				Solid state ^{119}Sn NMR
	Macrocyclic skeleton			Others	
	C_6H_4 (m, m, 4 H, 4 H)	CH (s, 2 H)	CH_3 (s, 12 H)	Aromatic ring	
$Sn(tmtaa)Cl_2$	7.20, 7.07	5.13	2.48		−432
1	7.22, 7.10	5.15	2.49		−432
2	7.10, 7.20	5.07	2.51		−436
3	7.20, 7.12	5.05	2.49	8.70 (s, 2H)	−415

[a] Chemical shifts are given in ppm for TMS. Measured in $CDCl_3$. Multiplicity of a proton signal is given in parentheses after δ value: s, singlet; m, multiplet.

[b] Chemical shielding is referenced to the ^{119}Sn resonance of tetramethyltin ($SnMe_4$) at 0 ppm and potassium stannate trihydrate ($K_2SnO_3 \cdot 3H_2O$) is used as the secondary reference, which chemical shielding appeared at −569 ppm.

of the chemical shift data concerns isotropic ^{119}Sn shift values measured in solution. Nevertheless, the complexes studied in our works do not have good solubility in non-polar or low polar solvents. Furthermore, in polar or high polar solvents, the axial substituents of these complexes will be substituted by solvent molecule and the coordination property of tin and ligands will perhaps change. Thus, the ^{119}Sn NMR spectroscopy was studied in solid state in our works. In the last few years, solid state ^{119}Sn NMR spectroscopy of various organotin complexes or other organometallic complexes containing tin has been studied [23–33]. Unfortunately, there are no studies available for tmtaa compound class. We were therefore anxious to record the solid state spectra of Sn(IV) in some tmtaa complexes with the expectation that such a study would reveal large anisotropies in their chemical shift tensors which would help elucidate the nature of the bonding in these complexes. High resolution solid state ^{119}Sn cross polarization magic angle spinning (CPMAS) NMR spectroscopy is an effective tool for detecting subtle details of structural and electronic properties of tin compounds [34,35].In our works, CPMAS NMR spectra were recorded at Larmor frequencies $\omega_0/2\pi$ of 111.9 MHz for ^{119}Sn. ^{119}Sn chemical shielding is referenced to the ^{119}Sn resonance of tetramethyltin ($SnMe_4$) at 0 ppm and potassium stannate trihydrate ($K_2SnO_3 \cdot 3H_2O$) is used as the secondary reference.

The data of Sn(tmtaa)Cl_2 and complexes **1**–**3**, obtained from solid state NMR experiments, are also given in Table 2. The singlet sharp signal of $K_2SnO_3 \cdot 3H_2O$ appeared at −569 ppm and broad peak of Sn(tmtaa)Cl_2 was observed at −432 ppm. Because of the analogous structures comparing with Sn(tmtaa)Cl_2, signals of **1** and **2** have similar shapes and appear at −432 and −436 ppm, respectively. ^{119}Sn chemical shift of **3** appears at −415 ppm, which is a little lower than those of Sn(tmtaa)Cl_2, **1** and **2**. Combining the discussion of the ^{1}H NMR spectra, we concluded the ^{1}H NMR data (part of methine) and the solid state ^{119}Sn NMR data in Fig. 2. It can be found that ^{1}H chemical shifts of Sn(tmtaa)Cl_2 and **1**–**3** appear at different positions. This may be due to the anisotropy effect of the triple bonds (C≡N) existing in the substituents of **1** and the NNN bonds existing in the substituents of **2**, and the ring current effect of aromatic ring existing in the substituent of **3**. Because of the different interactions between substituents and tmtaa unit, the ^{1}H chemical shifts of **1**–**3** shift to upfield or downfield comparing with Sn(tmtaa)Cl_2. However, ^{119}Sn chemical shifts of Sn(tmtaa)Cl_2, **1** and **2** appear at similar positions. This may be due to the electron donative ability of tmtaa group to the central metal which is greater than that of substituents to the central metal. Thus, though the substituents are different, ^{119}Sn chemical shifts of Sn(tmtaa)Cl_2, **1** and **2** are similar to each other because

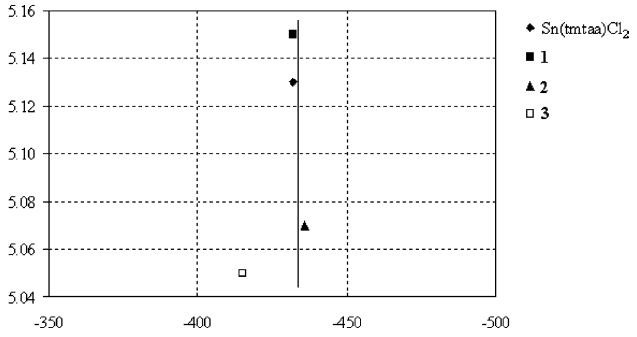

Fig. 2. ^{1}H NMR data (part of methine, vertical axis) and the solid state ^{119}Sn NMR data (horizontal axis) of Sn(tmtaa)Cl_2 and complexes **1**–**3**.

of the weak electron donative ability of the substituents to the central metal. Furthermore, being different from Sn(tmtaa)Cl_2, **1** and **2**, which have two homo-substituents, **3** has two hetero-substituents. The electron donative ability of two hetero-substitutes to tin atom in **3** is lower than those in Sn(tmtaa)Cl_2, **1** and **2**. Thus, the ^{119}Sn signal of **3** shifts a little downfield.

3.5. Crystal structures

The structural representation of **1** is shown in Fig. 3. Selected bond lengths and bond angles are given in Table 3. Notable features of the structural chemistry of tmtaa complexes are non-planar, saddle-shaped conformation and smaller N_4 coordination cavity 'hole size' than that of porphyrins and phthalocyanines. The structure determination of **1** reveals that it adopts *trans* six-coordinate configuration. The saddle shapes of the macrocyclic ligands are almost retained. The tin atom is

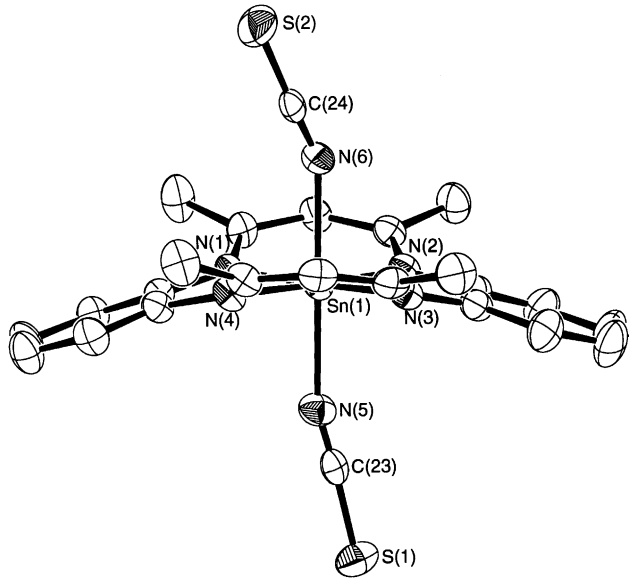

Fig. 3. ORTEP view of complex **1** with thermal ellipsoids shown at the 50% probability level. Hydrogen atoms have been omitted for clarity.

Table 3
Selected bond lengths (Å) and bond angles (°) for complex **1**

Bond lengths			
Sn(1)–N(1)	2.055(5)	Sn(1)–N(6)	2.207(6)
Sn(1)–N(2)	2.057(6)	N(5)–C(23)	1.058(9)
Sn(1)–N(3)	2.060(5)	N(6)–C(24)	1.096(8)
Sn(1)–N(4)	2.062(5)	C(23)–S(1)	1.666(8)
Sn(1)–N(5)	2.180(7)	C(24)–S(2)	1.620(8)
Sn(1)–N_4 least squares plane	0.041		
Bond angles			
N(5)–Sn(1)–N(6)	178.8(2)	N(5)–Sn(1)–N(3)	91.0(2)
Sn(1)–N(5)–C(23)	162.7(7)	N(5)–Sn(1)–N(4)	90.3(2)
Sn(1)–N(6)–C(24)	150.7(6)	N(6)–Sn(1)–N(1)	89.3(2)
N(5)–C(23)–S(1)	177.1(7)	N(6)–Sn(1)–N(2)	89.1(2)
N(6)–C(24)–S(2)	177.3(7)	N(6)–Sn(1)–N(3)	88.2(2)
N(1)–Sn(1)–N(3)	177.5(2)	N(6)–Sn(1)–N(4)	88.9(2)
N(2)–Sn(1)–N(4)	177.7(2)	N(1)–Sn(1)–N(2)	96.5(2)
N(5)–Sn(1)–N(1)	91.5(2)	N(2)–Sn(1)–N(3)	83.2(2)
N(5)–Sn(1)–N(2)	91.7(2)	N(3)–Sn(1)–N(4)	97.8(2)
		N(4)–Sn(1)–N(1)	82.3(2)

displaced from the N_4 plane towards the benzenoid face of tmtaa by 0.041 Å. In *trans* six-coordinate tmtaa germanium(IV) complex, Ge(tmtaa)$(NCS)_2$, the germanium atom is displaced from the N_4 plane towards the benzenoid face of the ligand by only 0.03 Å [11]. These small displacements may be a steric consequence of the *trans* geometry. The mean Sn–N bond distance in N_4 plane is 2.059 Å. It is a little longer than the mean Ge–N bond distance (1.926 Å) in N_4 plane in complex Ge(tmtaa)$(NCS)_2$ [11]. This may be due to the different hole sizes of **1** and Ge(tmtaa)$(NCS)_2$. In **1**, each NCS ligand adopts the most stereochemically favorable orientation with respect to the saddle-shaped macrocycle. The Sn(1)–N(5) distance (2.180 Å) on the benzenoid face is also shorter than the Sn(1)–N(6) distance (2.207 Å) on the opposite face of the molecule. Nitrogen atoms of NCS ligands and central metal are almost in the same line. N(5)–Sn(1)–N(6) bond angle is 178.8°. *Trans* axial nitrogen atoms are almost vertical to N_4 planes of the tmtaa ligands. NCS ligands keep their line characterization. N(5)–C(23)–S(1) and N(6)–C(24)–S(2) bond angles are 177.1° and 177.3°, respectively, whereas the Sn(1)–N(5)–C(23) and Sn(1)–N(6)–C(24) linkages are lightly bent (162.7° and 150.7°, respectively). All of these are similar to those of complex Ge(tmtaa)$(NCS)_2$ [11].

The ORTEP view of **3** is shown in Fig. 4. Selected bond lengths and bond angles are given in Table 4. One molecule of acetonitrile in the crystal lattice was observed. Because of the low reactivity of 2,4,6-trinitrophenolic anion, only one chloro atom which is on the opposite benzenoid face of the molecule was substituted from Sn(tmtaa)Cl_2. The chloro atom on the benzenoid face was retained, while the Sn(1)–Cl(1) distance (2.405 Å) became shorter than that in Sn(tmtaa)Cl_2 (2.453 Å) [6]. Because of two different substitutions in two sides of

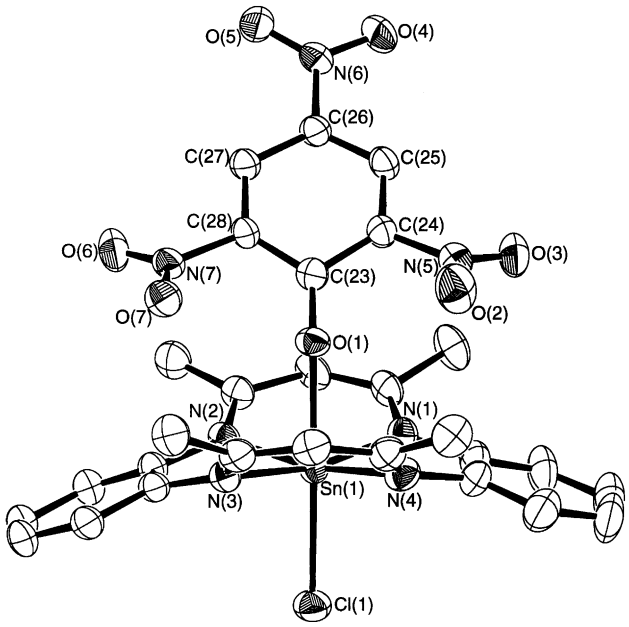

Fig. 4. ORTEP view of complex **3** with thermal ellipsoids shown at the 50% probability level. Hydrogen atoms have been omitted for clarity.

Table 4
Selected bond lengths (Å) and bond angles (°) for complex **3**

Bond lengths			
Sn(1)–N(1)	2.067(5)	N(5)–C(24)	1.467(8)
Sn(1)–N(2)	2.076(6)	N(5)–O(2)	1.215(9)
Sn(1)–N(3)	2.059(4)	N(5)–O(3)	1.230(8)
Sn(1)–N(4)	2.070(7)	N(6)–C(26)	1.459(8)
Sn(1)–Cl(1)	2.405(2)	N(6)–O(4)	1.232(7)
Sn(1)–O(1)	2.229(4)	N(6)–O(5)	1.205(7)
O(1)–C(23)	1.267(7)	N(7)–C(28)	1.472(7)
		N(7)–O(6)	1.218(8)
		N(7)–O(7)	1.220(8)
Sn(1)–N_4 least squares plane	0.208		
Bond angles			
Cl(1)–Sn(1)–O(1)	177.8(1)	O(2)–N(5)–O(3)	123.8(7)
Sn(1)–O(1)–C(23)	138.3(4)	O(2)–N(5)–C(24)	118.0(6)
N(1)–Sn(1)–N(3)	168.1(2)	O(3)–N(5)–C(24)	118.1(7)
N(2)–Sn(1)–N(4)	168.9(2)	O(4)–N(6)–O(5)	122.6(6)
Cl(1)–Sn(1)–N(1)	96.8(2)	O(4)–N(6)–C(26)	117.7(6)
Cl(1)–Sn(1)–N(2)	94.0(1)	O(5)–N(6)–C(26)	119.7(5)
Cl(1)–Sn(1)–N(3)	95.2(1)	O(6)–N(7)–O(7)	124.6(6)
Cl(1)–Sn(1)–N(4)	97.1(2)	O(6)–N(7)–C(28)	117.8(6)
O(1)–Sn(1)–N(1)	85.3(2)	O(7)–N(7)–C(28)	117.6(6)
O(1)–Sn(1)–N(2)	86.5(2)	O(1)–C(23)–C(24)	122.5(6)
O(1)–Sn(1)–N(3)	82.7(2)	O(1)–C(23)–C(28)	124.9(5)
O(1)–Sn(1)–N(4)	82.4(2)	C(24)–C(23)–C(28)	112.6(5)
N(1)–Sn(1)–N(2)	96.5(2)	N(5)–C(24)–C(23)	118.7(6)
N(2)–Sn(1)–N(3)	82.3(2)	N(5)–C(24)–C(25)	117.1(5)
N(3)–Sn(1)–N(4)	96.3(2)	C(23)–C(24)–C(25)	124.2(6)
N(4)–Sn(1)–N(1)	82.5(2)	N(6)–C(26)–C(25)	119.4(5)
		N(6)–C(26)–C(27)	118.8(6)
		C(25)–C(26)–C(27)	121.8(6)
		N(7)–C(28)–C(23)	119.7(5)
		N(7)–C(28)–C(27)	115.8(5)
		C(23)–C(28)–C(27)	124.5(5)

the molecule, the tin atom is displaced from the N_4 plane towards the benzenoid face of the ligand by 0.208 Å. It is obviously longer than that in other tmtaa Sn(IV) complexes (**1** and Sn(tmtaa)Cl_2[6]) containing two same substitutions. The mean Sn–N bond distance in N_4 plane is 2.068 Å. Because of the interaction of 2,4,6-trinitrophenolic group and tmtaa unit, the aromatic ring in the 2,4,6-trinitrophenolic group is not vertical to the N_4 plane of tmtaa. The dihedral angle of N_4 plane and aromatic ring is 45.0°. The plane of one nitro group containing N(6) is almost in the same plane of aromatic ring, their dihedral angle being 8.7°. However, the planes of other two nitro groups containing N(5) and N(7) are not in the same plane of aromatic ring and their dihedral angles are 38.0° and 31.2°, respectively. This may be due to the interaction of these two nitro groups and the methyl groups of the tmtaa unit.

4. Supplementary materials

Crystallographic data for the structural analysis have been deposited with the Cambridge Crystallographic Data Center, CCDC Nos. 192195 and 192196 for crystals of complexes **1** and **3**. Copies of the data may be obtained free of charge from The Director, CCDC, 12 Union Road. Cambridge, CB2 1EZ, UK (fax: +44-1223-336-033; E-mail: deposit@ccdc.cam.ac.uk or www: www.ccdc.cam.ac.uk).

Acknowledgements

We are grateful to the Center for Instrumental Analysis, Kyushu Institute of Technology, Japan for FAB mass spectra, ^{1}H NMR spectra, solid state ^{119}Sn NMR spectra, elemental analyses and X-ray structure determination.

References

[1] F.A. Cotton, J. Czuchajowska, Polyhedron 9 (1990) 2553.
[2] P. Mountford, Chem. Soc. Rev. 27 (1998) 105.
[3] D.A. Atwood, V.O. Atwood, A.H. Cowley, J.L. Atwood, E. Roman, Inorg. Chem. 31 (1992) 3871.
[4] G.R. Willey, M.D. Rudd, Polyhedron 11 (1992) 2805.
[5] D.A. Atwood, V.O. Atwood, A.H. Cowley, H.R. Gobran, J.L. Atwood, Inorg. Chem. 32 (1993) 4671.
[6] W.J. Belcher, P.J. Brothers, M.V. Land, C.E.F. Rickard, D.C. Ware, J. Chem. Soc., Dalton Trans. (1993) 2101.
[7] M.C. Kuchta, G. Parkin, Chem. Commun. (1996) 1669.
[8] M.C. Kuchta, G. Parkin, Polyhedron 15 (1996) 4599.
[9] W.J. Belcher, P.J. Brothers, A.P. Meredith, C.E.F. Rickard, D.C. Ware, J. Chem. Soc., Dalton Trans. (1999) 2833.
[10] X. Shen, K. Sakata, M. Hashimoto, Chem. Lett. (2001) 1326.
[11] X. Shen, K. Sakata, M. Hashimoto, Polyhedron 21 (2002) 969.
[12] SIR92: A. Altomare, M.C. Burla, M. Camalli, M. Cascarano, C. Giacovazzo, A. Guagliardi, G. Polidori, J. Appl. Cryst. 27 (1994) 435.
[13] DIRDIF94: P.T. Beurskens, G. Admiraal, G. Beurskens, W.P. Bosman, R. de Gelder, R. Israel, J.M.M. Smits, The DIRDIF-94 program system, Technical Report of the Crystallography Laboratory, University of Nijmegen, The Netherlands (1994).
[14] A.J. Blake, J.M. McInnes, P. Mountford, G.I. Nikonov, D. Swallow, D.J. Watkin, J. Chem. Soc., Dalton Trans. (1999) 379.
[15] L. Giannini, E. Solari, S.D. Angelis, T.R. Ward, C. Floriani, A. Chiesi-Villa, C. Rizzoli, J. Am. Chem. Soc. 117 (1995) 5801.
[16] G.I. Nikonov, A.J. Blake, P. Mountford, Inorg. Chem. 36 (1997) 1107.
[17] A.J. Blake, P. Mountford, G.I. Nikonov, D. Swallow, Chem. Commun. (1996) 1835.
[18] A. Klose, E. Solari, C. Floriani, S. Geremia, L. Randaccio, Angew. Chem., Int. Ed. 37 (1998) 148.
[19] A. Klose, E. Solari, C. Floriani, N. Re, A. Chiesi-Villa, C. Rizzoli, Chem. Commun. (1997) 2297.
[20] E.G. Jaeger, Z. Anorg. Allg. Chem. 364 (1969) 177.
[21] J.D. Kennedy, W. McFarlane, in: J. Mason (Ed.), Multinuclear NMR, Plenum, New York, 1987 (Chapter 4).
[22] B. Wrackmeyer, Annu. Rep. NMR Spectrosc. 38 (1999) 203.
[23] W. Plass, J.G. Verkade, Inorg. Chem. 32 (1993) 5153.
[24] C. Nedez, A. Choplin, F. Lefebvre, J.-M. Basset, Inorg. Chem. 33 (1994) 1575.
[25] S. Hayashi, A. Tanaka, M. Soma, Chem. Lett. (1995) 1081.
[26] B.E. Eichler, B.L. Phillips, P.P. Power, M.P. Augustine, Inorg. Chem. 39 (2000) 5450.
[27] Z. Lin, R. Rocha, J.D. Pedrosa de Jesus, A. Ferreira, J. Mater. Chem. 10 (2000) 1353.
[28] E. Siebel, R.D. Fischer, N.A. Davies, D.C. Apperley, R.K. Harris, J. Organomet. Chem. 604 (2000) 34.
[29] S.J. Garden, W.T.A. Harrison, R.A. Howie, H. Rufino, J.L. Wardell, J. Organoment. Chem. 619 (2001) 226.
[30] E.-M. Poll, J.-U. Schutze, R.D. Fischer, N.A. Davies, D.C. Apperley, R.K. Harris, J Organomet. Chem. 621 (2001) 254.
[31] M. Bechmann, X. Helluy, C. Marichal, A. Sebald, Solid State Nucl. Mag. 21 (2002) 71.
[32] J.C. Martins, F.A.G. Mercier, A. Vandervelden, M. Biesemans, J.-M. Wieruszeski, E. Humpfer, R. Willem, G. Lippens, Chem. Eur. J. 8 (2002) 3431.
[33] R.E. Dinnebier, P. Bernatowicz, X. Helluy, Main Group Met. Chem. 25 (2002) 115.
[34] D.C. Apperley, N.A. Davies, R.K. Harris, A.K. Birmah, S. Eller, R.D. Fischer, Organometallics 9 (1990) 2672.
[35] J.A. Davies, S. Dutremez, Coord. Chem. Rev. 114 (1992) 201.